

The dynamic stability analysis of guyed masts under random wind loads

Yan-Li He[†], Wu-Jun Chen[†] and Shi-Lin Dong[‡]

Research Center of Spatial Structures, Shanghai Jiao Tong University, Shanghai, 200030, P. R. China

Zhao-Min Wang[‡]

School of Civil Engineering, Tongji University, Shanghai, 200092, P. R. China

(Received July 18, 2000, Accepted March 22, 2002)

Abstract. On the basis of the first Lyapunov stability theory, this paper develops a dynamic stability criterion for elastic structural systems under arbitrary dynamic loads, and shows the stability criterion using energy variation. After the dynamic stability criterion is validated through a classic example, it is used for the dynamic stability investigation of practical guyed masts under random wind loads. The criterion is reliable, simple and of advantage for structures with large number of elements and nodes. The slack guys and internal resonance between guys and mast are two main factors which induces the dynamic instability of guyed masts, at the same time, some dynamic stability characteristics of guyed masts are found.

Key words: guyed masts; dynamic stability; random wind loads.

1. Introduction

Guyed masts consisting of slender masts and inclined prestressed guys often undergo large displacements due to wind loads, the failure probability of guyed masts under wind loads is very high in civil engineering field because their complex vibration behaviors are not well known. According to the data of near upon 100 collapsed guyed masts presented at the 17th conference of IASS guyed mast group, 50 percent of the collapses were caused by wind, hail and ice loads. Few of them were caused by very large wind, such as cyclone, most of them collapsed because of instability due to large amplitude vibration under low wind velocity.

There are many factors that can induce instability of guyed masts, the guys become slack, parametric resonance and ice coated galloping are key factors (He 2000). The paper lays emphasis on the theory analysis and numerical analysis about the first two factors causing instability of guyed masts.

[†] Associate Professor

[‡] Professor

2. The dynamic stability criterion of elastic structure system under arbitrary dynamic loads

Mathematically speaking, the dynamic stability is defined as the equation of motion being convergent (Shu 1989). It is impossible that the stability of a big structure is judged according to whether the equation of motion is convergent or not. For a structure, the essence of the instability is that the stiffness matrix of the structure becomes negative definite due to the geometric nonlinearities. Many scholars judged the stability through whether the stiffness matrix is positive definite or real part of eigenvalue is positive in the past (Komaraakul-Na-Nakorn 1990, Josef Fink 1992), this criterion cannot be well performed in the course of calculation. When the degrees of freedom of structure are very big, the criterion is often invalid due to numerical error and ill-conditioned matrix, so this stability criterion is limited to small structures or models.

The time history analysis is an effective method to judge the nonlinear stability of elastic structural systems (Zhang 1998). It is easy to obtain the time history response of structure in practical calculation, the energy variation can be obtained through the response of time history analysis. So, based on the Lyapunov stability theorem, the paper develops a new method to judge the stability through the energy variation.

The strain energy of structure can be expressed as

$$U_t = \sum_m \iiint_V \frac{1}{2} \{\sigma_t\}^T \{\varepsilon_t\} dV \quad (1)$$

$$\begin{aligned} U_{t+\Delta t} &= \sum_m \iiint_V \frac{1}{2} \{\sigma_{t+\Delta t}\}^T \{\varepsilon_{t+\Delta t}\} dV \\ &= \sum_m \iiint_V \frac{1}{2} (\{\varepsilon_t\}^T + \{\Delta\varepsilon\}^T) [D] (\{\varepsilon_t\} + \{\Delta\varepsilon\}) dV \end{aligned} \quad (2)$$

$$\begin{aligned} \Delta U &= U_{t+\Delta t} - U_t \\ &= \sum_m \iiint_V \{\sigma_t\}^T \{\Delta\varepsilon\} dV + \sum_m \iiint_V \frac{1}{2} \{\Delta\varepsilon\}^T [D] \{\Delta\varepsilon\} dV \end{aligned} \quad (3)$$

where, m is the number of elements, V is the volume of element, U_t is the structural strain energy at time t , $[D]$ is the elastic coefficient matrix, $\{\sigma_t\}$ is the element stress vector at time t , $\{\varepsilon_t\}$ is the element strain vector at time t , $\{\Delta\sigma\}$ is the element stress increment vector, $\{\Delta\varepsilon\}$ is the element strain increment vector and ΔU is the strain energy increment.

According to the first Castigliano theorem, the strain energy increment can be expressed in terms of stiffness matrix

$$\Delta U = \{u_t\}^T [K_c] \{\Delta u\} + \frac{1}{2} \{\Delta u\}^T [K_t] \{\Delta u\} \quad (4)$$

where, $[K_t]$ is the tangent stiffness matrix, $[K_c]$ is the secant stiffness matrix, $\{u_t\}$ is the displacement vector, $\{\Delta u\}$ is the displacement increment vector.

The complementary strain energy of structure can be written as

$$\begin{aligned} U_t^* &= [\{P_t\} - [M]\{\ddot{u}_t\} - [C]\{\dot{u}_t\}]^T \{u_t\} - U_t \\ &= \{F_t\}^T \{u_t\} - U_t \end{aligned} \quad (5)$$

$$\begin{aligned} U_{t+\Delta t}^* &= \{F_{t+\Delta t}\}^T \{u_{t+\Delta t}\} - U_{t+\Delta t} \\ &= \{F_{t+\Delta t}\}^T \{u_t\} + \{F_{t+\Delta t}\}^T \{\Delta u\} - U_{t+\Delta t} \end{aligned} \quad (6)$$

$$\begin{aligned} \Delta U^* &= U_{t+\Delta t}^* - U_t^* \\ &= (\{F_{t+\Delta t}\}^T - \{F_t\}^T) \{u_t\} + \{F_{t+\Delta t}\}^T \{\Delta u\} - (U_{t+\Delta t} - U_t) \end{aligned} \quad (7)$$

where, $[M]$ is the structural mass matrix, $[C]$ is the structural damping matrix, U_t^* is the complementary strain energy of structure at time t , ΔU^* is the complementary strain energy increment, $\{\ddot{u}_t\}$ is the acceleration vector, $\{\dot{u}_t\}$ is the velocity vector, $\{P_t\}$ is the vector of external loads and $\{F_t\}$ is the nodal equivalent static force vector.

Introducing the principle of virtual work, Eq. (7) can be written as

$$\begin{aligned} \Delta U^* &= \sum_m \iiint_V \{\sigma_{t+\Delta t}\}^T \{\varepsilon_t\} dV - \sum_m \iiint_V \{\sigma_t\}^T \{\varepsilon_t\} dV + \sum_m \iiint_V \{\sigma_{t+\Delta t}\}^T \{\Delta \varepsilon\} dV - (U_{t+\Delta t} - U_t) \\ &= \sum_m \iiint_V \{\Delta \sigma_t\}^T \{\varepsilon_t\} dV + \sum_m \iiint_V \{\sigma_t\}^T \{\Delta \varepsilon_t\} dV + \sum_m \iiint_V \{\Delta \sigma_t\}^T \{\Delta \varepsilon_t\} dV - (U_{t+\Delta t} - U_t) \end{aligned} \quad (8)$$

For the same way, the complementary strain energy increment can also be expressed with stiffness matrix

$$\begin{aligned} \Delta U^* &= U_{t+\Delta t}^* - U_t^* \\ &= \{u_t\}^T [K_t] \{\Delta u\} + \{u_t\}^T [K_c] \{\Delta u\} + \{\Delta u\}^T [K_t] \{\Delta u\} - (\Delta U) \\ &= \{u_t\}^T [K_t] \{\Delta u\} + \frac{1}{2} \{\Delta u\}^T [K_t] \{\Delta u\} \end{aligned} \quad (9)$$

The stiffness characteristics are implied in the energy variation seen from Eq. (4) and Eq. (9). The relationship between energy increment and the structural stiffness can also be obtained from Fig. 1.

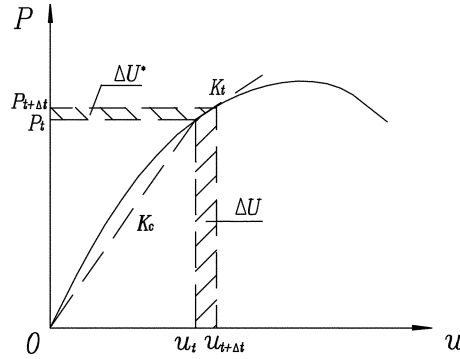


Fig. 1 Relationship between increment energy and the stiffness of structure

For the guyed masts with initial pre-stress, the relationship between energy increment and the stiffness of guyed mast structure can be expressed as

$$U_t = \sum_m \iiint_v \frac{1}{2} (\{\sigma_t\}^T - \{\sigma_0\}^T) (\{\epsilon_t\} - \{\epsilon_0\}) dV \quad (10)$$

$$\begin{aligned} U_t^* &= [\{P_t\} - [M]\{\ddot{u}_t\} - [C]\{\dot{u}_t\}]^T \{u_t\} - U_t \\ &= \{F_t\}^T \{U_t\} \end{aligned} \quad (11)$$

where, $\{\sigma_0\}$ is the initial stress vector and $\{\epsilon_0\}$ is the initial strain vector.

Combining Eq. (4) and Eq. (9),

$$\Delta U = \frac{\{u_t\}^T [K_c] \{\Delta u\} + 1/2 \{\Delta u\}^T [K_t] \{\Delta u\}}{\{u_t\}^T [K_t] \{\Delta u\} + 1/2 \{\Delta u\}^T [K_t] \{\Delta u\}} \Delta U^* \quad (12)$$

The relationship between the distribution of $(\Delta U, \Delta U^*)$ data points and the stability of the

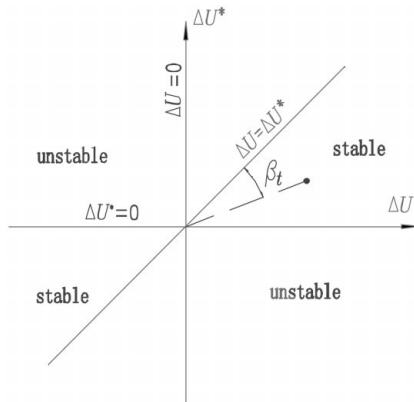


Fig. 2 Relationship between the distribution of $(\Delta U, \Delta U^*)$ data points and stability of structure

structure is demonstrated through a plot shown in Fig. 2, where, the horizontal axis represents ΔU , the vertical axis represents ΔU^* . For linear elastic structures, all the $(\Delta U, \Delta U^*)$ data points will scatter on the line $\Delta U = \Delta U^*$ according to Eq. (12); if the nonlinearity makes the structure stiffer, all the $(\Delta U, \Delta U^*)$ data points will deviate from the line $(\Delta U, \Delta U^*)$ to the line $\Delta U=0$; If the nonlinearity makes the structure softer, all the $(\Delta U, \Delta U^*)$ data points will deviate from the line $\Delta U = \Delta U^*$ to line $\Delta U^* = 0$. The phenomena emerge on the premise of which the structure is stable. If the structure is unstable, the all $(\Delta U, \Delta U^*)$ data will be chaotic (Nawrotzki 1994). Therefore, if all the $(\Delta U, \Delta U^*)$ data scattered on the second quadrant and the fourth quadrant in Fig. 2, the structural stiffness matrix is positive definite and the structure is stable. Once the structure become unstable, the $(\Delta U, \Delta U^*)$ data points will scatter on all four quadrants. So, the degree of stability of structure is judged by what angle the $(\Delta U, \Delta U^*)$ data deviate from the line $\Delta U = \Delta U^*$.

The degree of stability is defined as

$$DS(t) = \frac{\pi/4 - |\beta_t|}{\pi/4} \tag{13}$$

where, $|\beta_t|$ is the smallest angle between the line $\Delta U = \Delta U^*$ and the line which connect the origin of the axes $\Delta U, \Delta U^*$ with the datum $(\Delta U, \Delta U^*)$.

Then, the dynamic stability corresponding to the time history responses can be described as follows:

If the degree of stability is greater than or equal to zero at time t , i.e., $DS(t) \geq 0.0$, the structure is stable; If the degree of stability is less than zero at time t , i.e., $DS(t) < 0.0$, the structure is unstable.

The strain energy and complementary strain energy at any time t can be obtained from Eq. (1) and Eq. (5), respectively, then the increment strain energy and increment complementary strain energy can be obtained, the time history of degree of stability can be calculated using Eq. (13). Therefore, the stability in time history of elastic structures under arbitrary excitation is simply judged from the energy variation. The method is unlimited by the excitation style and type of instabilities.

3. Classical example analysis

Fig. 3 shows a planar truss made up of two hinged bars, the physical, geometry parameters and

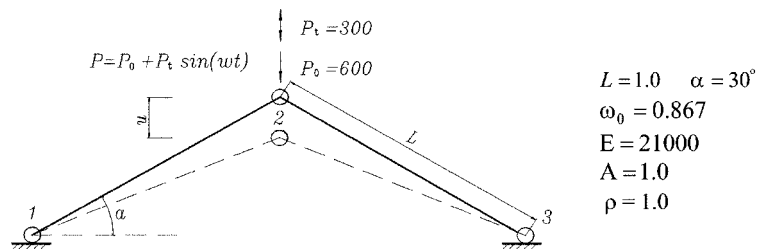


Fig. 3 Two hinged bars truss structure

loads are in constant units as shown in Fig. 3. The damping is neglected, and the material of all elements is elastic.

The dynamic nonlinear finite element equation of the structure is

$$[M]\{\ddot{u}_{t+\Delta t}\} + [C]\{\dot{u}_{t+\Delta t}\} + [K_t]\{u_{t+\Delta t}\} = \{P_{t+\Delta t}\} - \{R_t\} \quad (14)$$

where, $\{P_{t+\Delta t}\}$ is the vector of externally applied nodal forces at time $t+\Delta t$, and $\{R_t\}$ is nodal forces that correspond to element stresses.

The equation of motion is solved using the New-mark β difference method with $\beta=0.25$ and $\gamma=0.5$, the time step Δt is set as 0.2. The modified Newton method is used for nonlinear finite element iteration. The equations used in the modified Newton iteration are

$$[\tilde{K}_t]\{\Delta u_{t+\Delta t}\}^{i+1} = \{\Delta \tilde{P}_{t+\Delta t}\}^{i+1} \quad (15)$$

$$\{u_{t+\Delta t}\}^{i+1} = \{u_{t+\Delta t}\}_i + \{\Delta u_{t+\Delta t}\}^{i+1} \quad (16)$$

$$\text{where, } [\tilde{K}_t] = \frac{4}{\Delta t^2}[M] + \frac{2}{\Delta t}[C] + [K_t], \quad (17)$$

$$\begin{aligned} \{\Delta \tilde{P}_{t+\Delta t}\}^{i+1} = & \{P_{t+\Delta t}\} - \{R_{t+\Delta t}\}^i - [M] \left\{ \frac{4}{\Delta t^2} [\{u_{t+\Delta t}\}^i - \{u_t\}] - \frac{4}{\Delta t} \{\dot{u}_t\} - \{\ddot{u}_t\} \right\} \\ & - [C] \left\{ \frac{2}{\Delta t} [\{u_{t+\Delta t}\}^i - \{u_t\}] - \{\dot{u}_t\} \right\} \end{aligned} \quad (18)$$

The convergence criterion is

$$\|\{\Delta P_{t+\Delta t}\}^i\| \leq \text{RTOL} \|\{P_{t+\Delta t}\}\| \quad (19)$$

where, $\|\{\Delta P_{t+\Delta t}\}^i\|$ is out-of-balance force norm, and RTOL is convergence allowance.

The structure is resonated when the frequency of excitation is equal to the natural vibration frequency (the natural frequency is defined as the frequency of structure under static load P_0). The displacement time history response of the structure is shown in Fig. 4, the corresponding degree of stability time history shown in Fig. 5 is obtained according to the method presented above. The degree of stability DS is less than zero at 9.2s seen from Fig. 5, consequently, the structure becomes unstable according to degree of stability criterion.

In order to reflect characteristic and buckling path of the dynamic instability, the relationship between the equivalent static forces (defined by Eq. (5)) and vertical displacements of node 2 is shown in Fig. 6, the load-displacement relationship curve exhibits snap-through behavior of the instability of structure.

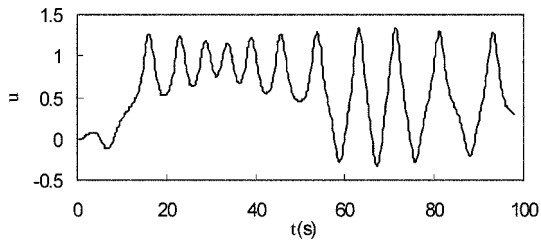


Fig. 4 Displacement time history of node 2

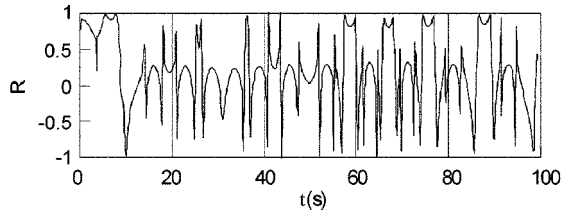


Fig. 5 Degree of stability time history of node 2

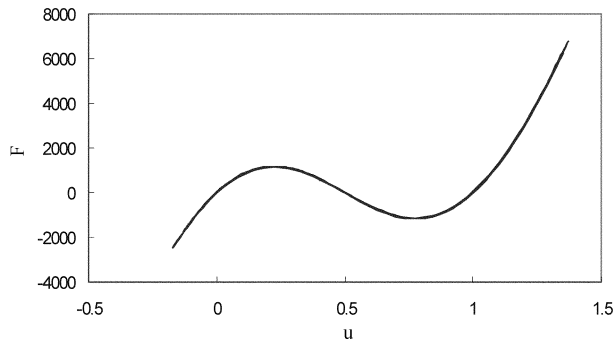


Fig. 6 Curve of nodal equivalent static force vs nodal displacement

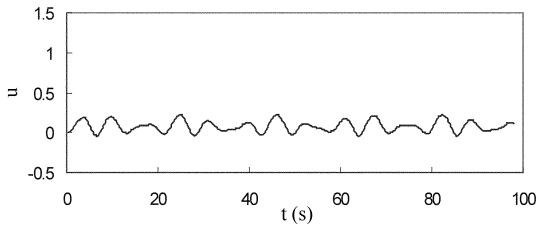


Fig. 7 Displacement time history of node 2

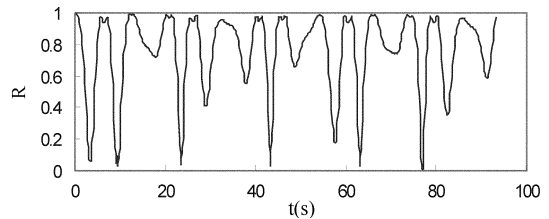


Fig. 8 Degree of stability time history of node 2

When the excitation frequency was changed to 1.2 Hz, the structure is forced vibrated. The displacement of structure under forced vibration is small, and the snap-through does not appear in the displacement time history shown in Fig. 7. The structure is stable as the degree of stability is always positive, $DS(t) \geq 0$, as shown in Fig. 8. In addition, the structure is stable judged from the relationship between the equivalent static forces and the vertical displacement of node 2 shown in Fig. 9.

It can be seen that the criterion is reliable and simple through the stability analysis of the classic example, and the criterion will be of many advantages for big structures.

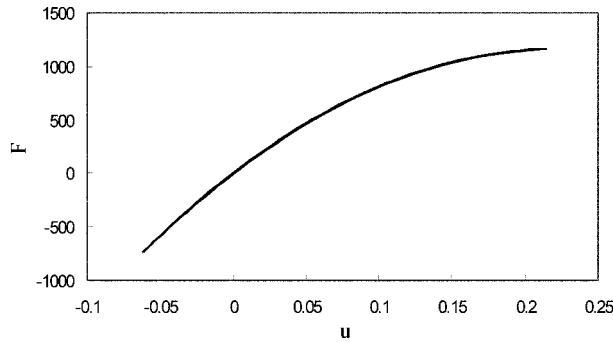


Fig. 9 Curve of nodal equivalent static force vs nodal displacement

4. Dynamic stability analysis of guyed masts

4.1. Example 1

The first example is a 150 m tall radio guyed mast with two stay levels guys and a ground terrain B (Chinese Building Loads Code). The tower consists of three-legged lattice steel mast and stayed by three pretension guy wires at each stay level as shown in Fig. 10.

The cross section of mast is an equilateral triangle with 1m side length, the web member is $\phi 102 \times 6$ and the chord member is $\phi 54 \times 4$ steel tube, the elastic modulus is $2.06 \times 10^5 \text{ N/mm}^2$. The guys are galvanized wire cables, having an elastic modulus equal to $1.20 \times 10^5 \text{ N/mm}^2$. The diameters of guys of upper and lower stay levels are 18.5 mm and 14.5 mm, respectively, the weight per unit length of guys of upper and lower stay levels are 56.3 N/m and 43.5 N/m, respectively. All guys are pre-stressed at 250 N/mm^2 , the breaking stresses of all guys are 1550 N/mm^2 .

The power spectrum of wind velocity is adopted as the one given by Davenport (Buchholdt 1985). It is

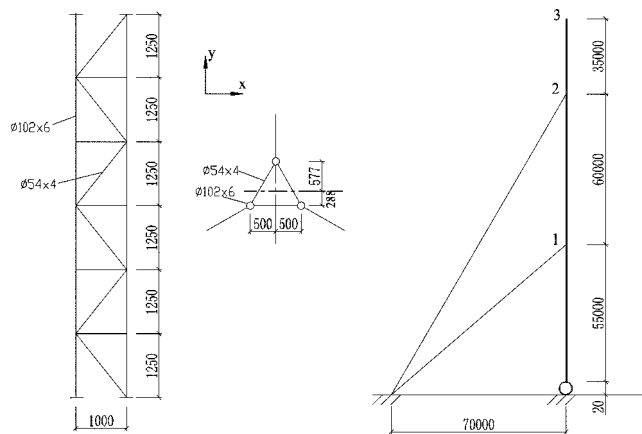


Fig. 10 Guyed mast structure (unit: mm)

$$S(\omega) = \frac{4k_r V_0^2 a^2}{\omega (1 + a^2)^{4/3}} \tag{20}$$

where, $a = 600\omega/\pi V_0^2$, ω is circular frequency, k_r is the terrain roughness, V_0 is the mean velocity, 28 m/s is used for the example to simulate the velocity. The wind loads acted on the structure along the y direction.

Only vertical correlativity of wind loads is considered by following equation

$$\sqrt{\text{Coh}(f)} = \exp\left\{\frac{-2f [10^2(z_i - z_j)^2]^{1/2}}{V_0(z_i) + V_0(z_j)}\right\} \tag{21}$$

where, f is frequency, $\sqrt{\text{Coh}(f)}$ is coherent factor.

The wind pressure of guys and masts are selected according to Chinese Building Loads Code, the structural damping factor is taken as 1%, the aerodynamic damping is ignored.

The mast is a lattice truss structure, the guy wires are taken as five-node truss elements (Bathe 1976). The wind-induced response analysis was performed with Newmark- β method, the time step is selected as 0.1s, the modified Newton Raphson scheme is also used for nonlinear iteration.

The dynamic stability of the guyed mast can be analyzed after the dynamic responses have been obtained. The degree of stability of the structure is found to be greater than zero seen from Fig. 11. Therefore, the guyed mast is stable when wind speed is 28 m/s. The displacement time history along y direction at node 2 is shown in Fig. 12, the time domain variations of the displacements and

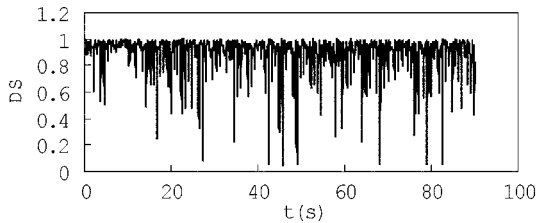


Fig. 11 Degree of stability of time history curve

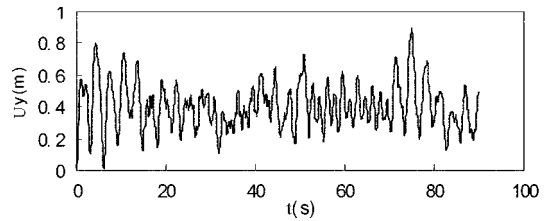


Fig. 12 Displacement time history at node 2 along y direction

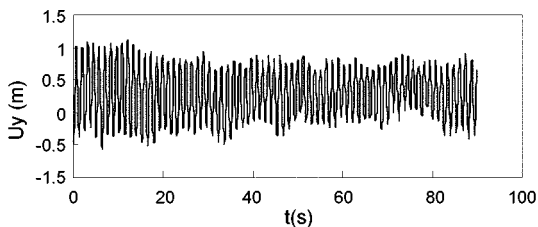


Fig. 13 Displacement time history of middle point of the upper stay level windward guy

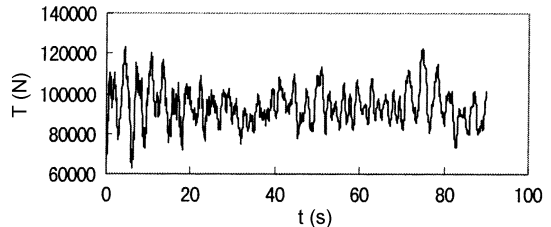


Fig. 14 Tension time history of the upper stay level layer windward guy

tension forces of the upper stay level guy are shown in Fig. 13 and Fig. 14, respectively.

4.2. Example 2

The parameters of mast and the wind loads that acted on the second example are same as that of the first example. The guys diameters of upper and lower stay level are, respectively, 12.5 mm and 11.5 mm, the initial stresses of the guys of upper and lower stay levels are both equal to 180 N/mm^2 , which means decrease in the lateral stiffness of the guyed mast.

The time history of the degree of stability is shown in Fig. 15, the displacement time history of node 2 is presented in Fig. 16, the time variations of the displacements and tension forces of guy's midpoint of upper stay level are shown in the Fig. 17 and Fig. 18, respectively.

The degree of stability is less than zero at time 2.6s as seen in Fig. 15, so the structure become unstable. The degree of stability is frequently less than zero after time 2.6s. Compared with the first example, the displacements of the masts and guys of the second example are much larger.

It is found that the slack guys(leeward) would cause the instability of guyed masts from preceding analysis. The case often appears during the erection of guyed masts, because the section area and initial stresses of temporary support cables are often small in the course of erection.

4.3. Example 3

The parameters of the mast of the third example are same as that of the first example. The guy's areas of upper layer and lower stay level are 108 mm^2 , their initial stresses are 250 N/mm^2 and 200 N/mm^2 , respectively. The wind load used for the third example acted along the x direction, with

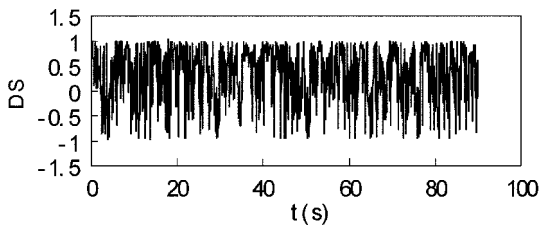


Fig. 15 Degree of stability time history

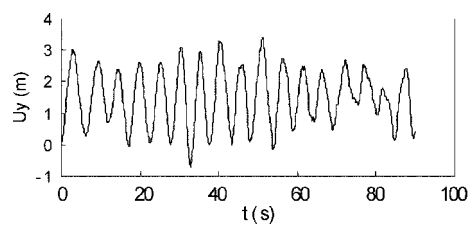


Fig. 16 Displacement time history of node 2 along y direction

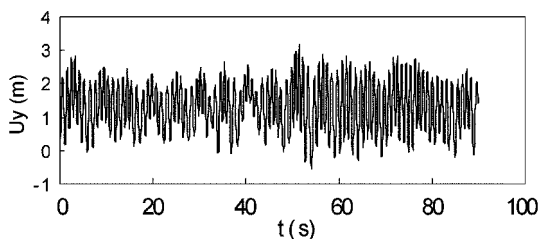


Fig. 17 Displacement time history of middle point of upper stay level windward guy

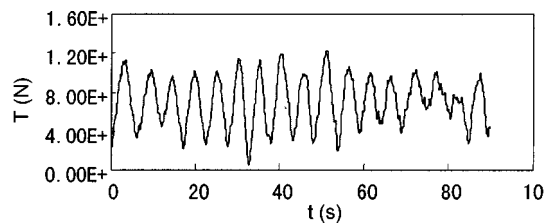


Fig. 18 Tension time history of upper stay level windward guy

a speed of 20 m/s.

For considering the internal resonance of guyed mast and interaction between the mast and the guys, (Warnitchai 1995), the total motions of guyed masts can be expressed as a sum of global and local motions. The global motions are 3-D motions of the structure where cables are treated as tendons, the effect of initial stresses should be included in the 3D-FEM formulation of structure; the local motions are motions of cables with two fixed ends.

The frequencies of the guyed mast are determined assuming that the structure vibrates about its deflected static equilibrium position under average wind speed in this paper. The lowest four frequencies of 3-D structure and cables with two fixed ends of the third example are listed in Table 1.

There are many frequency ratios of internal resonance between mast and guys in Table 1, Including, $2 f_{31} \cong f_{23}$, $3 f_{21} \cong f_{32}$, $f_{32} \cong f_{23}$, $2 f_{11} \cong f_{21}$, $3 f_{13} \cong f_{24}$. The first digit of subscript denotes the mast, upper layer guy or lower layer guy, the second digit of subscript refers to the number of frequency.

The time variations of internal resonance responses and the degree of stability of the guyed mast are shown in the following figures.

Table 1 Frequencies of mast, upper layer guys and lower layer guys

	Frequency of mast f_1 (Hz)	Frequency of upper stay level guys f_2 (Hz)	Frequency of lower stay level guys f_3 (Hz)
The first	0.3259	0.6573	0.9471
The second	0.6056	1.3032	1.8653
The third	0.8219	1.9266	2.7709
The forth	1.4453	2.5181	3.5062

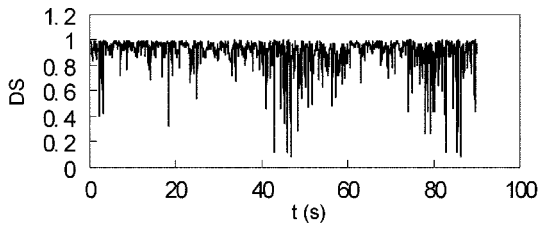


Fig. 19 Degree of stability time history

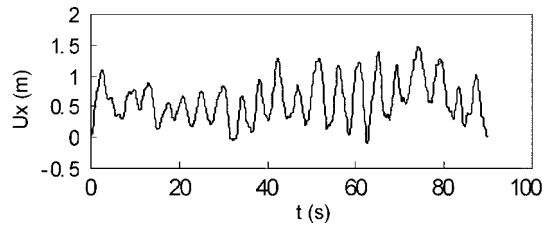


Fig. 20 Displacement time history at node 2 along y direction

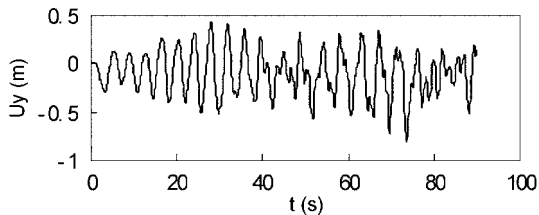


Fig. 21 Displacement time history at node 2 along x direction

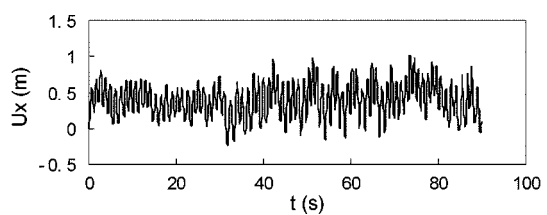


Fig. 22 Displacement time history of middle point of upper layer guy

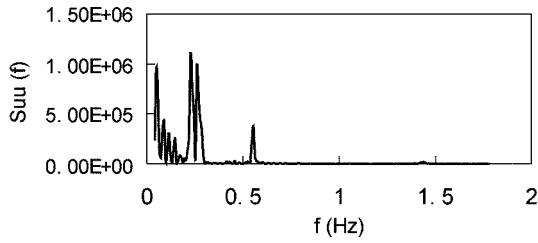


Fig. 23 Auto-spectrum of displacement of mast

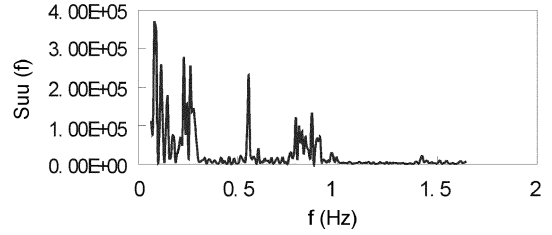


Fig. 24 Auto-spectrum of displacement of upper stay level guy along y direction

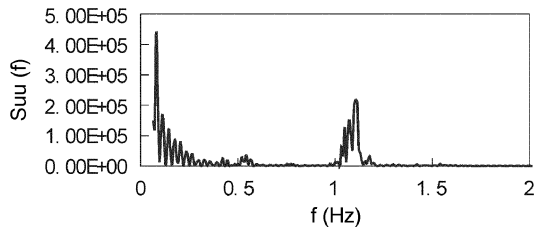


Fig. 25 Auto-spectrum of displacement of upper stay level guy along x direction

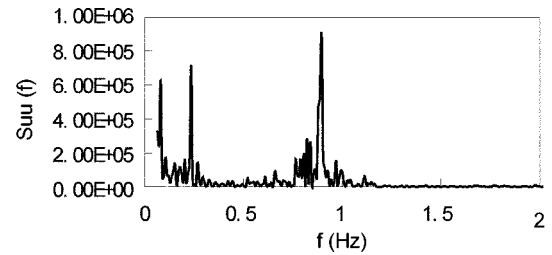


Fig. 26 Auto-spectrum of displacement of lower stay level guy along y direction

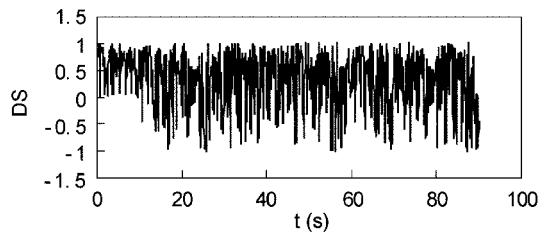


Fig. 27 Degree of stability time history

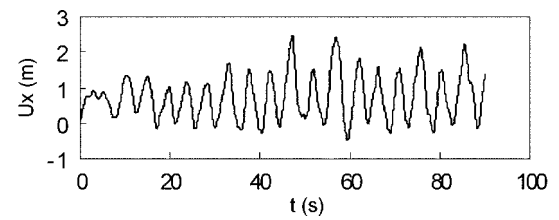


Fig. 28 Displacement time history at node 2 along x direction

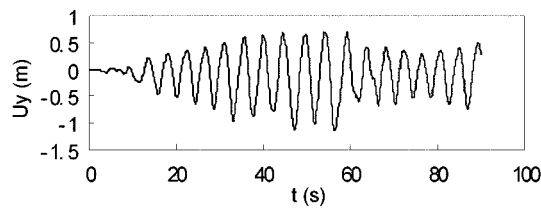


Fig. 29 Displacement time history at node 2 along y direction

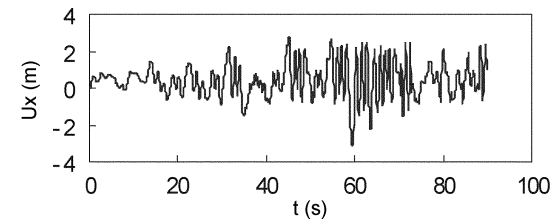


Fig. 30 Displacement time history of middle point of upper stay level guy

The degree of stability of the structure in time domain is always greater than zero seen from Fig. 19, consequently, the guyed mast under the wind loads is stable.

Many internal resonance phenomena can be found from displacement spectrum of the guyed mast shown in Fig. 23 to 26. The mast-guy coupling and guy-guy coupling become significant because these frequency tunings generate internal resonance, some high other frequencies make great contribution to the displacement response, and many coupling occur simultaneously seen from Fig. 24 and Fig. 26.

Keeping 20 m/s mean wind speed the frequency ratios between the mast and the guys are basically constant, only the fluctuating part of wind load increases to 1.4 times. The time history of degree of stability is shown in Fig. 27. The displacement time history curves of node 2 along x direction and along y direction are shown in Fig. 28 and Fig. 29, respectively. The displacement time history of guy's midpoint of upper stay level is shown in Fig. 30.

When the fluctuating component of wind loads increases, the guyed mast with frequency ratios of internal resonance is unstable at time 10.3s seen from Fig. 27. The type of instability is bending-torsion from deformation of whole guyed mast structure, the dynamic responses of the mast and guys increase largely due to the internal resonance, especially, the displacements along the direction perpendicular to wind become very large seen from Fig. 29.

A conclusion can be obtained through the dynamic stability analysis of the third example. The guy's amplitudes of guyed masts with frequency ratios of internal resonance, will increase when the dynamic wind speed increases because of the nonlinear coupling between the guys and mast. This coupling can induce large amplitude vibration of mast and guys, and would even cause the instability of whole guyed mast structure.

5. Conclusions

The stability criterion developed in the paper is reliable and simple through the stability analysis of a classic example and practical guyed masts, and has many advantages for stability analysis of big structures.

Guyed masts are nonlinear structures with large displacement, the essence of instability is that the stiffness matrix becomes negative definite due to the geometric nonlinearity. The guys becoming slack is one of factors which could cause the instability of guyed masts, the condition should be played high attention during the course of erection of guyed masts.

The large amplitude vibration of guys which is caused by internal resonance can result in large displacements of guyed mast through nonlinear coupling interaction, and would result in the instability of guyed masts (Warnitchai 1995). In practical guyed masts, the length and stress of guys are different, it is possible to form the frequency ratios of internal resonance between the guys and mast, which can cause the instability of guyed masts even the wind speed is not very large. So the internal resonance, especially the main parametric resonance, should be avoided in the design and erection of guyed masts.

References

- Bathe, K.J. and Wilson, (1976), *Numerical Method in Finite Element Analysis*, Englewood Cliffs.
- Buchholdt, H.A. (1985), *An Introduction to Cable Roof Structures*, Cambridge University Press.
- He, Y.L. (2000), "The dynamic stability analysis of guyed masts", Doctoral dissertation of Tongji University, Jan.

- (in Chinese).
- Josef Fink, (1992), "Dynamische und Aeroelastische Stabilitätsuntersuchung der Ausfachungsstäbe Von Hochspannungsmasten", Dissertationen der Technischen Universität Wien.
- Komarakul-Na-Kakorn, A. and Arora, J.S. (1990), "Stability criteria: A review", *Computer & Structure*, **37**(1), 35-49.
- Nawrotzki, P. (1994), "Numerical stability analysis of arbitrary structural responses", SFB 151-Bericht, Nr.24, Ruhr-University, Bochum.
- Shu, Z.Z. (1989), *Stability of Movement*, Southwest Jiao Tong University Press, Chengdu, (in Chinese).
- Wang, H.Q., (1992), *Nonlinear Vibration*, Higher Education Press, Beijing, (in Chinese).
- Warnitchai, P., Fujino, F. and Susumpow, T. (1995), "A nonlinear dynamic model for cables and its application to cable structure system", *Journal of Sound and Vibration*, **187**(4), 695-712.
- Zhang, Q.L. and Peil, U. (1998), "The dynamic stability analysis of elastic structure system under arbitrary dynamic loads", *Journal of Civil Engineering*, **31**(1), 26-32 (in Chinese).

CC